Male-biased islet β cell dysfunction is caused by the MODY MAFA S64F variant inducing premature aging and senescence

Emily M. Walker[1], Xin Tong[1], Jeeyeon Cha[1,2], Min Guo[1], Jin-Hua Liu[1], Sophia Yu[2], Donato Iacovazzo[3], Franck Mauvais-Jarvis[4], Sarah E. Flanagan[5], Márta Korbonits[3], John Stafford[1,2,6], David Jacobson[1], and Roland Stein[1,7]

[1]Department of Molecular Physiology and Biophysics, Vanderbilt University, Nashville, TN, USA

[2]Division of Diabetes, Endocrinology, and Metabolism, Department of Medicine, VUMC, Nashville, TN, USA

[3]Centre for Endocrinology, Barts and The London School of Medicine, Queen Mary University of London, EC1M 6BQ London, United Kingdom

[4]Section of Endocrinology and Metabolism, Department of Medicine, Tulane University Health Sciences Center, New Orleans, LA, USA

[5]Institute of Biomedical and Clinical Science, University of Exeter Medical School, EX2 5DW Exeter, United Kingdom

[6]Tennessee Valley Healthcare System, Veterans Affairs, Nashville, TN, USA

[7]Corresponding author: Roland.Stein@Vanderbilt.Edu; Tel: 615-322-7026

Abstract

A heterozygous missense variant in the islet β-cell-enriched MAFA (Ser(S)64Phe(F)) transcription factor was identified in humans who developed either diabetes or insulinomatosis, with males more prone to diabetes. This mutation engenders increased stability to the normally unstable MAFA protein. To obtain insight into how this impacts β cell function, we developed a mouse model expressing S64F MafA and found sex-dependent phenotypes, with heterozygous mutant males displaying impaired glucose tolerance while females were slightly hypoglycemic and had improved blood glucose clearance. Only heterozygous males showed higher MafA protein levels, which preceded the onset of glucose intolerance and sex dependent variations in expression of genes involved in aging, DNA damage, calcium signaling, and senescence. Changes in islet calcium handling and signs of aging and senescence processes were validated in male animals. Together, these results implicate accelerated islet aging and senescence in promoting diabetes in male human S64F MAFA carriers.

Introduction

The large V-Maf Avian Musculoaponeurotic Fibrosarcoma transcription factor MafA is a pancreatic β-cell-enriched protein essential for activating rodent transcriptional programs to promote cell maturation and glucose-stimulated insulin secretion (GSIS) (Artner et al., 2008; Artner et al., 2010; Hang and Stein, 2011; Hang et al., 2014; Zhang et al., 2005). The presence of MafA in only insulin^{+} β cells during islet cell development and postnatally distinguishes it from other important islet cell-enriched regulators (Golson and Kaestner, 2017; Hang and Stein, 2011; Pan and Wright, 2011; Shih et al., 2013). For example, transcription factors such as Pdx1 and Nkx6.1, which are expressed earlier and more broadly, also have a profound impact on pancreas organogenesis, islet β cell function, and whole body glucose homeostasis in mice (Madsen et al., 1997; Pan and Wright, 2011). Pdx1 is present in both the exocrine and endocrine pancreas during development and then principally in islet β cells postnatally (Pan and Wright, 2011), while Nkx6.1 is found in endocrine progenitors and is later restricted to β cells (Golson and Kaestner, 2017; Hang and Stein, 2011; Pan and Wright, 2011; Shih et al., 2013). In contrast, mice lacking MafA (i.e. *MafA*$^{-/-}$ (Zhang et al., 2005), *MafA*$^{\Delta panc}$ (Artner et al., 2010; Hang et al., 2014), *MafA*$^{\Delta}$ (Cyphert et al., 2019; Luan et al., 2019)) have normal pancreas formation and have a relatively subtle influence on postnatal physiology, primarily compromising GSIS in a sex-independent manner. However, MafA has been proposed to play a distinct late role in postnatal islet β cell maturation, in part supported by observations demonstrating that inducing MafA expression levels in normally non-glucose responsive and MafA^{Low} neonatal rat islets increases GSIS (Aguayo-Mazzucato et al., 2011), while compromising levels reduces mouse (Artner et al., 2010; Cyphert et al., 2019; Hang et al., 2014; Luan et al., 2019; Zhang et al., 2005) and human (Guo et al., 2013) β cell activity. A key regulatory role is also implied by the ability of many islet-enriched transcription factors to coordinately stimulate *MafA* gene transcription, including Pdx1 and Nkx6.1. (Raum et al., 2006; Raum et al., 2010)

Expression of the other large Maf family member produced in the islet, MafB, differs from MafA in being expressed in both murine α- and β-cells developmentally (Cyphert et al., 2019; Hang and Stein, 2011), then postnatally only in α cells and a subpopulation of β cells during pregnancy (Banerjee et al., 2016; Cyphert et al., 2019). Moreover, genetic studies have demonstrated that MafB is dispensable in regulating adult murine islet β cell function, except during pregnancy (Banerjee et al., 2016; Cyphert et al., 2019). MafA expression during mouse β cell development compensates for the absence of MafB, although glucagon secretion from islet α cells is compromised (Cyphert et al., 2019). In addition, mis-expressing MafB in *MafA*$^{\Delta panc}$ β cells cannot rescue MafA function (Cyphert et al., 2019). Collectively, these results illustrate similarities and differences between MafA and MafB in expression and function in rodent islet cells.

While most islet-enriched transcription factors are produced in an analogous fashion in rodents and humans, there are unique differences in the temporal and islet cell type-specific expression pattern of the human MAFA and MAFB proteins. In humans, MAFA protein is not found in the β cell until about 10 years of age, while MAFB is present throughout the lifespan of the human insulin^{+} cell population (Cyphert et al., 2019; Dai et al., 2012). These observations imply that humans have at least two postnatal MAFA^{+} β cell populations capable of maintaining euglycemia, represented by the juvenile (i.e. <10 years old and MAFA^{Low}:MAFB^{+}) and post-juvenile (~10+ years old and MAFA^{High}:MAFB^{+}) periods. In fact, independent studies have established distinct molecular and functional properties of these temporally produced human cell populations (Arda et al., 2016; Arrojo et al., 2019; Camunas-Soler, 2019), and an association between MAFA levels and adult islet β cell functional heterogeneity (Chen et al., 2019). MAFA and MAFB levels are reduced in type 2 diabetic (T2D) islets (Guo et al., 2013), and (at least) MAFA is particularly sensitive to oxidative stress and glucotoxic conditions (Harmon et al., 2005). While the role of MAFA or MAFB has not been analyzed directly in intact human islets, both are

required for GSIS in the human EndoC-βH1 β cell line (Scharfmann et al., 2014; Scoville et al., 2015). Moreover, we have recently shown that MAFB is essential to insulin production in human embryonic stem cell derived β cells (Russell, 2020), which is in stark contrast to its dispensable role in rodents (Banerjee et al., 2016; Cyphert et al., 2019). These findings highlight species-specific differences in MAFA and MAFB production and islet cell distribution, likely implying that the homodimeric MAFB activator and the MAFA:MAFB heterodimeric activator provide unique functional characteristics to human islet β cells.

Individuals carrying a heterozygous mutation causing the substitution of the conserved Serine at position 64 with a Phenylalanine (S64F) in the MAFA transactivation domain develop either insulinomatosis, a condition of hyperinsulinemic hypoglycemia caused by multiple insulin-secreting neuroendocrine tumors, or diabetes with a mean age at diagnosis of 38 years (Iacovazzo et al., 2018). These results demonstrate that MAFA is a causative gene for Maturity Onset Diabetes of the Young (MODY), a disease predominately driven by mutations in essential islet-enriched transcription factors (Barbetti and D'Annunzio, 2018). Of note, diabetes is prevalent in male S64F MAFA carriers (i.e. 3:1) while insulinomatosis is more common in female carriers (4:1) (Iacovazzo et al., 2018). *In vitro* analysis demonstrated that S64F prevents phosphorylation at S65 in MAFA, which profoundly increases the stability of the normally unstable MAFA protein by affecting processes necessary for ubiquitin-mediated degradation (Iacovazzo et al., 2018).

Due to the rare nature of S64F MAFA-mediated diseases and difficulty of performing mechanistic studies in a human context, we used CRISPR-based mutagenesis to establish a mouse model with the same pathogenic single base pair substitution (C>T) as human carriers. Diabetes-related phenotypes were specifically associated with male *MafA*$^{S64F/+}$ heterozygous mice by 5 weeks of age, which were manifested as glucose intolerance and impaired insulin secretion due to reduced glucose-stimulated β cell Ca^{2+} influx. These changes were preceded by an overt, but transient increase in MafA protein levels in islet β cells at 4 weeks. In addition, the functional deficiencies in male *MafA*$^{S64F/+}$ islet β cells accompanied the induction of markers of

DNA damage, cell cycle exit, senescence, and the senescence-associated secretory phenotype (SASP) at 5 weeks. These findings were in contrast to heterozygous mutant female mice, which not only had lower fasting blood glucose levels and improved glucose clearance, but also did not display any of the overt aging and senescence signatures of the male variants. Taken together, these results strongly suggest the induction of effectors of senescence and premature aging in islet β cells by S64F MAFA causes diabetes in male human carriers.

Methods

Animals

S64F MafA animals were generated using CRISPR/Cas9 targeting at the University of Michigan Transgenic Core in the C57BL/6J mouse strain. Viable animals and progeny were screened for the appropriate mutation by DNA sequencing (Molecular Resource Center, University of Tennessee Health Science Center). Wild-type littermates were used as controls. *MafA*$^{S64F/+}$ were born at normal Mendelian ratios while homozygous *MafA*$^{S64F/S64F}$ variants were not (see below). All animal studies were reviewed and approved by the Vanderbilt University Institutional Animal Care and Use Committee. Mice were housed and cared for according to the Vanderbilt Department of Animal Care and the Institutional Animal Care and Use Committee of Animal Welfare Assurance standards and guidelines.

Intraperitoneal glucose and insulin tolerance testing

Glucose tolerance testing was performed on WT and *MafA*$^{S64F/+}$ mice (n = 4-16) given an intraperitoneal injection of D-glucose (2 mg/g body weight) prepared in sterile PBS (20% w/v) after a 6-hour fast. Insulin tolerance tests were conducted by intraperitoneal injection of 0.5 IU/kg body weight insulin (Novolin, regular human insulin, recombinant DNA origin) into mice (n=3-5) fasted for 6 hours. Blood glucose was measured using a FreeStyle glucometer (Abbott Diabetes Care) before (0 minutes) and at 15, 30, 60, and 120 minutes following injection. Serum insulin was measured by radioimmunoassay at the Vanderbilt Hormone Assay and Analytical Services Core using blood collected following the 6-hour fast. Serum testosterone was measured by the University of Virginia Center for Research in Reproduction Ligand Assay and Analysis Core.

Glucose-stimulated hormone secretion

WT and *MafA*$^{S64F/+}$ mouse (n = 3-6) islets were isolated using standard islet isolation conditions and used in hormone secretion assays as described previously (Cyphert et al., 2019). The outcome was presented as the fold change between the percentage of secreted insulin or glucagon relative to the total insulin or glucagon content at either 2.8 or 16.7 mmol/L glucose. Islet insulin and glucagon content was presented as the concentration of insulin or glucagon per DNA content (Quant-iT™ PicoGreen™, Invitrogen) in each reaction (ng/ng DNA).

Tissue preparation and immunostaining

WT and *MafA*$^{S64F/+}$ pancreata were fixed in 4% (v/v) paraformaldehyde, embedded in either Tissue-Plus O.C.T. (Thermo Fisher Scientific) or paraffin wax, and sectioned to 6 μm thickness. Immunofluorescent images were obtained using the Zeiss Axio Imager M2 widefield microscope with ApoTome. Immunofluorescence staining was performed as previously described with the antibodies listed in Supplementary Table 1. Islet β- and α- cell areas were determined as described previously (Banerjee et al., 2016). Pancreatic section results (n=3-4) were scanned using a ScanScope CS scanner (Aperio Technologies, Vista, CA). Images from each experiment were processed with ImageScope Software (Aperio Technologies, Vista, CA). Islet β- and α-cell areas were calculated as the ratio of the insulin- or glucagon-positive area to total pancreas area (eosin stained). The TUNEL assay was performed using an *in situ* cell death detection kit (Roche, #11684795910).

RNA sequencing and analysis

RNA was isolated from WT and *MafA*$^{S64F/+}$ islets (n=4-5) using the RNAqueous total RNA isolation kit (Ambion; Thermo Fisher), and then analyzed on an Agilent 2100 Bioanalyzer. Only samples with an RNA Integrity Number >8.0 were used for library preparation. cDNA libraries

were constructed and paired-end sequencing of 4-5 replicates was performed on an Illumina NovaSeq6000 (150 nucleotide reads). The generated FASTQ files were processed and interpreted using the Genialis visual informatics platform (https://www.genialis.com). Sequence quality checks were determined using raw and trimmed reads with FastQC (http://www.bioinformatics.babraham.ac.uk/projects/fastqc), and Trimmomatic (Bolger et al., 2014) was used to trim adapters and filter out poor-quality reads. Trimmed reads were then mapped to the University of California, Santa Cruz, mm10 reference genome using the HISAT2 aligner (Kim et al., 2015). Gene expression levels were quantified with HTSeq-count (Anders et al., 2015), and differential gene expression analyses performed with DESeq2 (Love et al., 2014). Poorly expressed genes, which had expression count summed over all samples of <10, were filtered out from the differential expression analysis input matrix. Quantitative real-time PCR expression analysis of selected candidates was performed using cDNAs produced from the iScript cDNA Synthesis Kit (Bio-Rad) in a LightCycler 480 system (Roche) with primers provided in Supplementary Table 2.

Islet cytosolic calcium imaging

Approximately 60 WT and *MafA*$^{S64F/+}$ islets from at least 6 female and male mice were analyzed with the ratiometric Ca^{2+} indicator fura-2-acetoxymethylester (Fura-2 AM) (Life Technologies). Islets were maintained in 5 mM glucose for 30 min prior to measuring 11 mM glucose-induced Ca^{2+} oscillations and depolarization-activated Ca^{2+} influx with 30 mM KCl. Islets were loaded with 2 μM Fura-2 AM for 20 min, washed, transferred to a hand-made agarose gel small-volume chamber in a glass bottom dish. Images were taken using a Nikon Eclipse TE2000-U microscope equipped with an epifluorescence illuminator (SUTTER, Inc), a CCD camera (HQ2; Photometrics, Inc), and Nikon Elements software (NIKON, Inc) as described before (Dadi et al., 2015).

Senescence-associated β-galactosidase (SA-β-gal) staining

WT and *MafA*$^{S64F/+}$ pancreata were snap frozen in O.C.T. and cryosections were prepared at 16 μm thickness. SA-β-gal activity staining was performed at pH 6.0 (Kurz et al., 2000) using a commercial kit (Cell Signaling, #9860). To compare the intensity of SA-β-gal staining, sections from different genotypes and ages were processed on the same slide. Staining reactions were stopped after an 18-hour wash in PBS (pH 7.4). Slides were then subject to immunostaining for insulin by fixing in 4% paraformaldehyde for 45 minutes, permeabilized with Tris-buffered saline with 0.2% Triton-X-100 for 15 minutes, blocked in 2% normal donkey serum/1% BSA in PBS and incubated overnight with guinea pig anti-insulin (1:500, Abcam) at 4□C. HRP-conjugated secondary antibodies were then incubated on slides for 1-hour and detected with the DAB+ chromogen kit (DAKO). After washing, slides were mounted and imaged by brightfield microscopy. SA-β-gal+ islet numbers were analyzed on ImageJ.

Ovariectomy methods

Wildtype and *MafA*$^{S64F/+}$ female mice underwent ovariectomy at 3 weeks to remove the contribution of endogenous ovarian hormones and prevent completion of sexual maturity (Martinez et al., 2012). Mice were anesthetized with 1-5% inhaled isoflurane, and placed prone on a heating pad to maintain their body temperature at 37^0 C. The mice received subcutaneous ketofen at 5-10 mg/kg prior to surgery and post-operatively for two days for pain relief. Intraperitoneal ceftriaxone at 20-40 mg/kg was given once intraoperatively for infection prophylaxis. After adequate anesthesia and analgesia, a midline 1.5 cm incision was made along the shaved mid-dorsal surface of the mouse. Within the retroperitoneal cavity, the ovaries were

located and ligated. The incision was closed using surgical staples, which were removed on post-operative day three. Mice were housed singly during recovery and regrouped post-operatively.

Glycogen storage assay

Liver and gastrocnemius muscle from WT and *MafA*$^{S64F/+}$ mice (n=5) were collected and flash frozen in liquid nitrogen. Tissue was homogenized with a Dounce homogenizer prior to determining glycogen content using a Glycogen assay kit (Cayman Chemical) according to the manufacturer's protocol.

Statistical Analysis

Statistical significance was determined using the two-tailed Student *t* test. Data are presented as the mean ± SEM. A threshold of $P < 0.05$ was used to declare significance.

Results

Male *MafA*$^{S64F/+}$ mice are glucose intolerant due to impaired insulin secretion

Since MafA is a primary regulator of glucose clearance and insulin secretion in islet β cells (Hang and Stein, 2011), *MafA*$^{S64F/+}$ and wild-type (WT) littermates were subjected to glucose tolerance testing (GTT) and fasting blood glucose measurements at various postnatal time points. While both male and female heterozygous animals had improved glucose clearance at 4 weeks, females were modestly hypoglycemic (**Figure 1A**). Notably, male heterozygous mutant animals developed persistent glucose intolerance beginning at 5 weeks of age, while females continued to have improved glucose tolerance and lower fasting blood glucose levels (**Figure 1A**). GTT results were stably maintained in male and female *MafA*$^{S64F/+}$ mice (**Supplemental Figure 1**). The sex-dependent male phenotype was even more penetrant in homozygous *MafA*$^{S64F/S64F}$ mutants, as males displayed overt diabetes with elevated fasting glucose levels that progressively worsened (**Supplemental Figure 2A**, **B**). In contrast, the phenotype of homozygous females was much more variable (**Supplemental Figure 2C**). Because of the generally poor survival of homozygous mutants postnatally (**Supplemental Figure 2D**), all of the remaining experimentation was performed with male and female *MafA*$^{S64F/+}$ mice.

Ex vivo GSIS was impaired in 5-week-old male *MafA*$^{S64F/+}$ islet β cells (**Figure 1B**), although insulin content was decreased in both male and female mutant islets (**Figure 1C**). The mutant female mice appear to have lower fasting blood glucose levels due to increased serum insulin levels (**Figure 1A, D**). Because of the counter-regulatory effects of insulin on glucagon hormone secretion (Franklin et al., 2005), we considered that glucose-regulated glucagon levels might be altered in *MafA*$^{S64F/+}$ mice. However, there was neither a sex-dependent impact on low glucose-induced glucagon secretion nor a change in glucagon content (**Supplemental Figure**

3A, **B**). In addition, α cell area was decreased in both male and female heterozygous islets, although this was variable among animals (**Supplemental Figure 3C**).

MafA$^{S64F/+}$ insulin^{+} β cell area was reduced in both sexes (**Figure 1E**), which may be due to the lower cell proliferation rate of *MafA*$^{S64F/+}$ relative to WT littermates (**Supplemental Figure 4**). In addition, the changes in blood glucose levels were not attributable to differences in peripheral tissue insulin sensitivity or glucose uptake as insulin tolerance tests and glycogen storage were both unchanged (**Supplemental Figure 5A, B**). Animal growth rates were also not appreciably altered as assessed by body weight (**Supplemental Figure 5C**).

Because the sex hormones estradiol and testosterone impact islet cell function (Gannon et al., 2018), we questioned whether these hormones influenced the sex-biased phenotypes in *MafA*$^{S64F/+}$ mice. Both sexes achieved puberty appropriately with normal fertility (data not shown). Female *MafA*$^{S64F/+}$ mice were ovariectomized to investigate whether estrogen was regulating mutant sex-biased activity. Ovariectomy produced glucose intolerance in 4- and 5-week-old WT female mice., In contrast, glucose tolerance was unaffected by ovariectomy in age-matched female *MafA*$^{S64F/+}$ mice (**Supplemental Figure 6A,** data not shown). These results indicate that the S64F MafA mutation is dominant over the effect of estrogen-deficiency on glucose intolerance. Furthermore, testosterone levels were not altered markedly in males (**Supplemental Figure 6B**). Unfortunately, we were unable to develop experimental conditions to reduce testosterone levels in 4-week-old male *MafA*$^{S64F/+}$ mice, although testosterone levels at both 4 and 5 weeks of age were similar to females (**Supplemental Figure 6B**). The low relative levels of testosterone produced in these peri-pubertal mice presumably explains why manipulating levels was so difficult and lowers the likelihood of this hormone influencing MafA^{S64F} actions.

Collectively, these data strongly suggested that S64F MafA regulates male and female islet β cells through mechanisms that are both common and distinct, yet not principally controlled by sex hormone function.

MafA protein levels are transiently and profoundly upregulated prior to the changes in glucose clearance in male *MafA*$^{S64F/+}$ islet β cells

By blocking phosphorylation at S65 and subsequently the phosphorylation at S61, T51, T57, and S49 by glycogen synthase kinase 3, the S64F MAFA protein did not undergo ubiquitin-mediated protein degradation and its stability dramatically increased in the human EndoC-βH1 β cell line (Han et al., 2007; Iacovazzo et al., 2018; Rocques et al., 2007). Consequently, we predicted that MafA protein levels would also be increased in *MafA*$^{S64F/+}$ β cells. Surprisingly, we only found elevated MafA protein immunostaining intensity in male *MafA*$^{S64F/+}$ islets at 4 weeks of age (**Figure 2A**), one week prior to the onset of glucose intolerance (**Figure 1A**). In contrast, MafA protein levels were not increased in female *MafA*$^{S64F/+}$ β cells at 4 weeks or any other analyzed time point in relation to WT controls (**Figure 2B**). However, there was a roughly 3- to 5-fold decrease in *MafA* transcript levels at 4 and 5 weeks of age in both male and female *MafA*$^{S64F/+}$ islets compared to WT littermates (**Figure 2C**). The reduction in *MafA* gene expression indicates that MafA^{S64F} is acting in an autoregulatory manner by binding at the conserved MafA binding site within the 5'-flanking sequences of the Region 3 transcription control domain (Artner et al., 2008; Artner et al., 2010; Scoville et al., 2015).

Glucose and potassium chloride (KCl) stimulated Ca^{+2} handling are altered in both male and female *MafA*$^{S64F/+}$ islets

To provide an unbiased and comprehensive perspective on how MafA^{S64F} influences islet β cell gene expression, bulk RNA-sequencing was performed on isolated islets from 5-week-old WT and *MafA*$^{S64F/+}$ male and female mice. Female heterozygous islets had 736 differentially expressed (DE) genes compared with female WT islets (i.e. 337 up and 399 down) while males had 2410 DE genes (2031 up and 379 down) compared with male WT islets (**Figure 3A**). There

were also genes (i.e. 391) that were regulated in a similar manner between sexes, which were revealed by gene ontology analysis to include factors associated with Ca^{2+} and potassium channels important in controlling β cell function (**Figure 3B, C**). Notably, voltage-dependent Ca^{2+} channels genes as well as other genes important to ion influx were also specifically up-regulated in male *MafA*$^{S64F/+}$ islets (**Figure 3D**). Because glucose-induced elevations of cytoplasmic Ca^{2+} result in insulin release (Bergsten et al., 1994), WT MafA and *MafA*$^{S64F/+}$ islet Ca^{2+} handling was monitored in response to glucose stimulation and KCl-induced depolarization.

As expected from the diminished GSIS response of male *MafA*$^{S64F/+}$ islets (**Figure 1B**), their Ca^{2+} entry was significantly blunted relative to the WT islets in response to 11 mM glucose stimulation (**Figure 4A**; represented by red trace in left panel and termed "non-responders"). The glucose-stimulated Ca^{2+} oscillation pattern that is responsible for pulsatile insulin secretion was also significantly diminished in *MafA*$^{S64F/+}$ islets (**Figure 4A**). In contrast, there appeared to be two distinct islet populations in female *MafA*$^{S64F/+}$ animals with different glucose-stimulated Ca^{2+} responses. One was similar to male *MafA*$^{S64F/+}$ islets in having a very limited initial glucose response and minimal oscillatory behavior (i.e. **Figure 4A,** dark green representative trace in right panel and labeled as "non-responders"). However, the remaining islets had more subtle decreases in the initial response to 11 mM glucose, and subsequently oscillate with higher frequency but equivalent amplitude to WT islets (**Figure 4A;** "responders", teal representative trace in right panel). The average peak amplitude of the initial glucose-induced Ca^{2+} response was reduced in all male and female *MafA*$^{S64F/+}$ islets (**Figure 4B**). This suggests that the *MafA*$^{S64F/+}$ female islet "responders" population is able to compensate for the "non-responders" and maintain glucose tolerance in *MafA*$^{S64F/+}$ female mice, which would be predicted because only roughly 20% of functional β cell mass is required to maintain physiological levels (Gale, 2002).

Male and female *MafA*$^{S64F/+}$ islets also had disparate Ca^{2+} responses to KCl-mediated depolarization. The KCl-induced Ca^{2+} influx (ΔCa^{2+} after KCl application divided by baseline Ca^{2+}) was significantly reduced in male *MafA*$^{S64F/+}$ islets when compared to WT male islets. Interestingly,

however, the female *MafA*$^{S64F/+}$ islets showed greater KCl-induced Ca^{2+} influx when compared to WT female islets, which was observed for both glucose-stimulated Ca^{2+} "responders" and "non-responders" (**Figure 4C** and **Supplemental Figure 7)**. Importantly, female *MafA*$^{S64F/+}$ islets also showed greater baseline (5 mM glucose) Ca^{2+} than WT female (**Figure 4D**), which suggests that the elevated basal islet Ca^{2+} levels results in the fasting hypoglycemia and increased fasting insulin levels observed in female *MafA*$^{S64F/+}$ mice (**Figure 1**).

Only male *MafA*$^{S64F/+}$ islets express markers of accelerated cellular senescence and aging

Because 5-week-old male *MafA*$^{S64F/+}$ islet β cells were not only defined by a major non-responsive Ca^{2+} responsive population(s) (**Figure 4A,B**) but also by glucose intolerance (**Figure 1A**), we focused our attention on identifying additional determinants to poor β cell function. In addition to the previously illustrated gene expression alterations involved in Ca^{2+} signaling (Index ranking #6, **Figure 5A**), 5-week-old male *MafA*$^{S64F/+}$ RNA-Seq data revealed upregulation of many metabolic pathway genes implicated in cellular aging (e.g. Index ranking pathways #4, 6, and 8) and senescence (e.g. Index ranking pathways #1, 2, 3, 5, 6, 7 and 8 in **Figure 5A**) (Basisty et al., 2018; Campisi and d'Adda di Fagagna, 2007; Coppe et al., 2010; Franceschi et al., 2018; Greenhill, 2019; Kabir et al., 2016; Mancini et al., 2012; Martin and Bernard, 2018). Furthermore, the preponderance of upregulated genes detected by RNA-Seq indicates that MafA^{S64F} is acting as a dominant activator in (at least) male *MafA*$^{S64F/+}$ islet β cells (**Figure 3A**).

Significantly, cellular senescence is a durable, cell cycle arrest response seen during development, organismal aging, and cell maturation to regulate cell fate specification and tissue patterning (e.g. islet β cells (Campisi, 2014; Gorgoulis et al., 2019; Helman et al., 2016; Herranz and Gil, 2018)). It is also induced in a variety of disease states and primarily serves as a stress response to many internal and external insults (Gorgoulis et al., 2019; Herranz and Gil, 2018). The importance of premature aging and senescence in driving male *MafA*$^{S64F/+}$ β cell dysfunction was supported by the many genes associated with these responses, including those controlling

Ca^{+2} signaling (**Figure 3D**), aging (**Figure 5B**), DNA damage response (**DDR**, **Figure 5C**), the senescence-associated secretory phenotype (**SASP**, **Figure 5D**), and cytokine-cytokine receptor interactions (**Figure 5E**).

As expected, the expression of candidate genes linked to aging and senescence were increased in 5-week-old male *MafA*$^{S64F/+}$ islets (**Figures 5F**). Importantly, none of these features were seen in the *MafA*$^{S64F/+}$ females (**Figures 3D** and **5B-F**). Additionally, we identified increased immunostaining for cell cycle arrest and senescence marker p21 (Fang et al., 1999) and DNA damage marker P53 binding protein-1 (53BP1) (Schultz et al., 2000) in 5-week-old *MafA*$^{S64F/+}$ male islets, but not female (**Supplemental Figure 9A**, **B**). However, apoptosis was not induced in response to DNA damage in either male or female *MafA*$^{S64F/+}$ male islets, as concluded by the inability to detect islet TUNEL^{+} cells between 4-7 weeks of age (**Supplemental Figure 10, data not shown**). Increased endogenous senescence-associated β-galactosidase (SA-β-gal) staining was also detected in male *MafA*$^{S64F/+}$ islets at levels comparable to aged mice (**Figure 6A, C**). Notably, SA-β-gal was undetectable in male *MafA*$^{S64F/+}$ islets prior to compromised β cell function at 4 weeks, nor in female mutant islets (**Figure 6A-C**). Together, these results illustrate a novel sex-dependent pathophysiology in *MafA*$^{S64F/+}$ of accelerated β cell aging and senescence that contributes to the males' decreased GSIS.

Discussion

Post-translation modifications of the MAFA protein are very important in regulating its activity, stability and cellular localization (Guo et al., 2009; Guo et al., 2010; Han et al., 2007; Iacovazzo et al., 2018; Rocques et al., 2007). Here we have developed a mouse model of the human pathogenic S64F MAFA variant to gain insight into why affected heterozygous human carriers produce, in a sex-biased manner, distinctly different pathophysiological outcomes in their late 30's of MODY or insulinomatosis (Iacovazzo et al., 2018). This mutation blocks a key priming phosphorylation event at S65 which normally directs post-translational modifications impacting MAFA protein stability (Guo et al., 2009; Han et al., 2007; Rocques et al., 2007), transactivation (Han et al., 2007; Rocques et al., 2007), oncogenesis (Rocques et al., 2007) and DNA binding (Guo et al., 2010). These modifications are coupled to two antagonistic regulatory processes: increased transactivation activity and ubiquitin-mediated degradation (Rocques et al., 2007) illustrating that impeccable regulation of this protein is linked to islet β cell health. The physiological outcomes of *MafA*$^{S64F/+}$ mice appear to mimic the outcomes expected in human subjects, with glucose intolerance almost exclusively in males and improved glucose clearance and hypoglycemia in females. Because compromised voltage-gated Ca^{2+} channel triggering of glucose-induced insulin secretion in *MafA*$^{S64F/+}$ males appeared to be caused by an inactivated β cell population, we focused on understanding how regulation was impacted in this context. Significantly, dysfunctional islet β cells in male *MafA*$^{S64F/+}$ mice were associated with advanced cellular aging and senescence, whereas *MafA*$^{S64F/+}$ females were not. Notably, independent reports have also linked pathologic, senescent β cell populations with Type 1 Diabetes (T1D) and T2D islet dysfunction (Aguayo-Mazzucato et al., 2019; Thompson et al., 2019).

Earlier *in vitro* analysis demonstrated that the S64F *MAFA* mutation converted this normally unstable protein ($t_{1/2}$ ~30 min) to a very stable form ($t_{1/2} \geq$ 4 hours) (Iacovazzo et al., 2018). However, both male and female *MafA*$^{S64F/+}$ mice had similar improvements in glucose

tolerance at 4 weeks, prior to overt and transient elevation in protein levels in just males (**Figures 1 and 2**). Notably, this increase in MafA^{S64F} protein levels induced glucose intolerance by 5 weeks of age in males, while females continued to be modestly hypoglycemic with improved glucose clearance. Deficiencies in whole body glucose homeostasis were even more apparent in male homozygous *MafA*$^{S64F/S64F}$ mice, manifested as an explicit elevation in fasting blood glucose levels and glucose intolerance which worsened with age.

The changes in male and female *MafA*$^{S64F/+}$ β cell activity were maintained throughout the period of analysis despite the presence of WT-like protein levels after 5 weeks. Human MAFA protein levels were also unchanged upon comparing immunohistochemical staining in islets to the insulinomatosis β cell mass in S64F MAFA patients (Iacovazzo et al., 2018). However, we propose that MafA^{S64F} is more abundantly and persistently produced than WT MAFA throughout the lifetime of the β cell, as supported by 3- to 5-fold lower *MafA* mRNA levels in male and female MafA$^{S64F/+}$ islets in relation to the WT islets (**Figure 2C**). Our examination of ovariectomized female *MafA*$^{S64F/+}$ mice suggested that the estrogen sex hormone did not have a direct regulatory role, so it is presently unclear what factors are controlling the sex-biased phenotypes of MafA^{S64F} mutant mice. Since S64F MAFA-induced disease is not observed until around 38 years of age (Iacovazzo et al., 2018), we also believe that neither estrogen nor testosterone are impactful to the disease process in humans. Instead we propose that future efforts should focus on determining if sex chromosome gene expression is influential, such as the X chromosome-linked candidate genes found differentially expressed in 5-week-old *MafA*$^{S64F/+}$ male islets but not females compared to their respective WT controls (**Supplemental Figure 11**).

Bulk RNA-Seq analysis of 5-week-old male and female *MafA*$^{S64F/+}$ mice islets illustrated both similarities in how β cell identity and ion channel functional genes were dysregulated (Figure 3, Supplemental Figure 8). For example, expression of several markers of β cell maturation were diminished in both *MafA*$^{S64F/+}$ male and female islets (Supplemental Figure 8), including the Mnx1 (Pan et al., 2015) and Pdx1 transcription factors as well as well the UCN3 neuropeptide (van der

Meulen et al., 2015). In addition, we also observed clear male-biased differences in Ca^{+2} signaling pathway-related gene expression (**Figure 3**). While all male 5-week-old mutant islets appear to have severely blunted glucose-induced Ca^{+2} responses (termed non-responders in **Figure 4**), females contained both responder and non-responder islets. Presumably, responder islets mediate the high basal glucose-induced insulin secretion properties characteristic of female *MafA*$^{S64F/+}$ islets (**Figure 4A and D**, **Figure 1D**), while downstream effectors of Mnx1 and Pdx1 activation that are involved in cell signaling (e.g. *Gcgr, Glp1r*), secretion (*Syt2, Ucn3, Ins1, Ins2*) and ion channel activity contribute to β cell non-responder dysfunction (Blum et al., 2014; Gilbert and Blum, 2018; Jacobson and Shyng, 2020; Kalwat and Cobb, 2017). Because of the disparity of the Ca^{+2} signaling changes in female *MafA*$^{S64F/+}$ islets, we focused on determining possible mechanisms contributing to the MafA^{S64F} induced diabetic phenotype in males. Future single cell sequencing efforts could reveal the factors regulating the distinct responder and non-responder islet β cell populations controlling MafA^{S64F} females as well as their homogeneity in male non-responder islets. Importantly, our results clearly show that the many gene products associated with male *MafA*$^{S64F/+}$ β cell inactivity are not made in female variants.

Our results have demonstrated that MafA^{S64F} produces premature aging and senescence signatures in only male β cells (**Figures 5 and 6**). Unlike the temporary arrest of cellular quiescence, senescence is thought to be irreversible and refractory to mitogenic stimuli. Senescent cells undergo a progression of changes after initial insult: early initiation of cellular arrest by activation of cell cycle inhibitors (i.e. p53, p21 and/or p16 (**Supplemental Figure 9**), among others) and activation of DDR responses in an attempt to regain homeostasis (Gorgoulis et al., 2019; Herranz and Gil, 2018). DDR can be characterized by markers such as phosphorylated histone H2AX and 53BP1 recruitment to chromatin (**Supplemental Figure 9**). Progression to senescence involves chromatin remodeling to influence gene expression, metabolism, autophagy and SASP, with release of a heterogeneous mix of SASP effector proteins influencing neighboring cells in a non cell-autonomous manner (Gorgoulis et al., 2019; Herranz

and Gil, 2018). Terminal senescence from persistent damage involves autocrine and paracrine SASP amplification, loss of nuclear integrity and diversification of the phenotype (Gorgoulis et al., 2019). Notably, senescence-associated SA-β-gal staining was not induced in 4-week-old *MafA*$^{S64F/+}$ β cells, the time point just prior to detection of glucose intolerance (**Figures 1 and 6**).

Ultimately, senescent cells become resistant to apoptosis by up-regulation of anti-apoptotic proteins (such as those in the BCL2 family) and are often cleared by immune cells (Gorgoulis et al., 2019; Herranz and Gil, 2018). Interestingly, effective clearance of β cells is not apparent in *MafA*$^{S64F/+}$ male islets as we see accumulation of senescent cells, and there was no evidence of β cell death (**Figure 6**, **Supplemental Figure 10,** data not shown). Senescent cells can play a causal role in aging and aging-related pathology (van Deursen, 2014) and targeted removal of senescent cells can improve health span and reduce the incidence of aging-related diseases (Baker et al., 2016; Baker et al., 2011; Chang et al., 2016; Childs et al., 2016). Indeed, independent studies have shown removal of the rare, senescent β cells in mouse models of T1D and T2D helps restore β cell function and glucose homeostasis *in vivo*. These senescent β cells showed distinct SASP signatures depending on modeling context (T1D vs. T2D) (Aguayo-Mazzucato et al., 2019; Thompson et al., 2019) and these signatures were also species-dependent such that SASP mediators from mouse/human islets were not able to induce senescence in human/mouse islets, respectively (Aguayo-Mazzucato et al., 2019; Thompson et al., 2019). Significantly, as divergent regulation of metabolism between sexes in aging and disease is increasingly recognized (Sampathkumar et al., 2019), MAFA^{S64F} may provide a penetrant model to study sex-dependent effects on β cell health.

Human and rodent islets differ substantially in architecture, cell composition, proliferative capacity, islet amyloid formation, antioxidant enzyme levels, and, most significantly for the results described herein, MAFA and MAFB transcription factor expression (Bosco et al., 2010; Brissova et al., 2005; Butler et al., 2007; Cabrera et al., 2006; Dai et al., 2012; Fiaschi-Taesch et al., 2010; Henquin et al., 2006; Tyrberg et al., 2001). Because MafA is expressed at the onset of rodent β

cell formation during embryogenesis but not until 10 years of age in humans (Cyphert et al., 2019; Dai et al., 2012; Hang and Stein, 2011), we appreciate that some of the observations made in *MafA*$^{S64F/+}$ mice will not be relevant to the human disease. For example, since β cell proliferation ceases in humans prior to MAFA expression (Cyphert et al., 2019; Dai et al., 2012; Hang and Stein, 2011), the decreased islet cell proliferation observed in male and female *MafA*$^{S64F/+}$ mice will not be observed in humans. We also did not expect to find that *MafA*$^{S64F/+}$ male mice would manifest the overt fasting hyperglycemia seen in affected humans (Iacovazzo et al., 2018), since only one of the seven human MODY transcription factors has a phenotype in heterozygous mice comparable to human carriers (i.e. Pdx1 (Ahlgren et al., 1998)). MafA^{S64F} presumably represents another example of species-specific differences in how gene dosage of critical regulatory gene variants impacts islet cell health.

It is also likely that the human MAFA^{S64F}:MAFB heterodimeric activator will impart a unique influence on β cells compared to the mouse MafA^{S64F}:MafA homodimeric activator (Cyphert et al., 2019; Hang and Stein, 2011), which may explain why neuroendocrine tumors and overt hypoglycemia was not observed in aged MafA$^{S64F/+}$ mice (data not shown). Notably, MAFB was recently shown to be essential for the formation of human embryonic derived β cells and insulin production (Russell, 2020), whereas there is no phenotype associated with the loss of MafB in mouse islet β cells (i.e. except during pregnancy (Conrad et al., 2016)). We believe that it will be important to extend the analysis of MAFA^{S64F} control to human β cells, which could include transplantation of human islets expressing this transcription factor variant into immunocompromised mice to directly determine its effect *in vivo*. Such studies should generate keen insight into unique, species-specific, age-dependent and sex-biased molecular and genetic mechanisms controlling human islet β cell activity.

Acknowledgements

This research was performed using resources and/or funding provided by the NIDDK-grants to R.S. (DK090570), E.M.W. (F32 DK109577), J.C. (T32DK007061), F.M.J. (DK074970 and DK107444), J.S. (DK109102), J.S. (NHLBI, HL144846), D.J. (DK097392), and the Vanderbilt Diabetes Research and Training Center (DK20593). X.T. was supported by a JDRF Fellowship (3-PDF-2019-738-A-N), J.C. by Harrison Society funds, D.I. by a George Alberti Research Training Fellowship funded by Diabetes UK (16/0005395), and F.M.J. also by a U.S. Department of Veterans Affairs Merit Review Award (BX003725). Imaging was performed with NIH support from the Vanderbilt University Medical Center Cell Imaging Shared Resource (National Cancer Institute grant CA-68485; NIDDK grants DK20593, DK58404, and DK59637; Eunice Kennedy Shriver National Institute of Child Health and Human Development grant HD-15052; and National Eye Institute grant EY08126). Islet hormone analysis was performed in the Vanderbilt University Medical Center Islet Procurement and Analysis Core (NIDDK grant DK20593) and Vanderbilt University Neurochemistry Core (NICHD grant U54 HD083211).

All authors have no conflict of interest to declare.

Author Contributions

E.M.W., X.T., J.C. and R.S. designed the initial experiments. E.M.W., X.T., J.C., M.G. and J.-H.L. executed and analyzed the experiments with input from S.Y., D.I., S.F, M.K., S.K., F. M-J., D.J. and R.S. The manuscript was principally written by E.M.W., X.T., J.C. and R.S., although all authors have reviewed versions. R.S. is the guarantor of this work and, as such, had full access to all the data in the study and takes responsibility for the integrity of the data and the accuracy of the data analysis.

Figure Legends

Figure 1: Male but not female *MafA*$^{S64F/+}$ mice become glucose intolerant between 4 and 5 weeks of age. A) Fasted male and female animals underwent intraperitoneal glucose tolerance tests at 4 and 5 weeks of age. Male heterozygous (termed Het) *MafA*$^{S64F/+}$ mice (red line) had improved glucose clearance at 4 weeks but become glucose intolerant by 5 weeks. Female Het mice (teal line) had significantly lower fasting blood glucose levels and improved glucose clearance at both time points. B) High glucose stimulated insulin secretion in isolated islets was impaired in male Het samples at 5 weeks. Islets were incubated with 4.6 mM (low, LG) or 16.8 mM (high, HG) glucose for 1-hour. C) Islet insulin content was decreased in both Het males and females. Levels were normalized to B) insulin content and C) DNA content. D) Serum insulin levels (ng/mL) were increased in 6-hour fasted female Het animals while male Het levels were unchanged. E) Male and female islet β cell area was reduced at 5 weeks in *MafA*$^{S64F/+}$ mice and even further by 7 weeks. The area was calculated by dividing the total Insulin^{+} area by the total pancreatic area (eosin staining) in pancreas sections obtained every 50 μm multiplied by 100 to obtain percent (%). *$p<0.05$; **$p<0.01$; ***$p<0.001$.

Figure 2: MAFA protein levels were transiently upregulated at 4 weeks in male *MafA*$^{S64F/+}$ islets. A) Immunostaining over the course of 3, 4, 5, 6 and 7 weeks revealed that MAFA protein intensity only increased at 4 weeks of age in male S64F MafA Het islets. B) In contrast, MAFA staining intensity was unchanged between female Het and WT islets. C) *MafA* mRNA levels were significantly reduced at 4 and 5 weeks in both male and female Het islet samples. Fold change shown relative to male WT islets. *$p<0.05$.

Figure 3: Male and female *MafA*$^{S64F/+}$ islet β cells regulate a common and distinct set of genes associated with calcium (Ca^{+2}) and potassium (K) channel activity. A) The Venn diagram illustrates the total number of RNA-Seq identified genes up- or down-regulated between 5-week-old WT and Het islets. B) Gene Ontology (GO): Molecular function analysis of the 391 genes commonly up- or down-regulated in S64F MafA Het islets revealed multiple channel activity pathways. C) Heat maps showing channel gene expression changes common between male and female Het islets, and (D) calcium signaling pathway genes uniquely increased in male Het islets by KEGG analysis (also see Figure 5A). FDR<0.05.

Figure 4: Glucose-induced Ca^{+2} oscillations and KCl-induced Ca^{2+} responses are altered in *MafA*$^{S64F/+}$ islets. A) Representative Fura2 traces show loss of the β cell-induced Ca^{+2} oscillations by 11 mM glucose (G) in 5-week-old male S64F MafA Het islets (red line and termed non-responders). Female Het islets had two different functionally responsive β cell populations ("responders," teal line; "non-responders," green line). B) Quantitation of male (left) and female (right) islets showed reduced cytoplasmic Ca^{+2} following stimulation with 11 mM glucose. The average peak amplitude was quantitated by dividing the first peak ΔCa^{2+} after 11mM glucose application by the baseline response. C) The Ca^{+2} response to 30mM KCl is reduced in male S64F MafA Het islets but increased in female mutant islets. Representative traces of this experiment are shown in Supplemental Figure 7. D) Female S64F MafA Het islets have increased baseline Ca^{+2} at 5mM compared with WT islets (right) indicating enhanced secretion, while male variant islets do not (left). **p<0.01; ***p<0.001.

Figure 5: Male *MafA*$^{S64F/+}$ islets display aging, DDR, SASP, and cytokine gene pathway signatures. A) KEGG analysis of the 1842 genes specifically upregulated in 5-week-old male S64F MafA Het islets. Heat maps reveal male S64F MafA Het islets have increased expression of pathway genes associated with B) aging, C) DDR, D) SASP, and E) cytokine-cytokine receptor

interactions. FDR<0.05. F) qRT-PCR confirmation of pathway gene changes in 5-week-old male *MafA*$^{S64F/+}$ islets.

Figure 6: Senescence generated SA-β-gal staining was only increased in dysfunctional male *MafA*$^{S64F/+}$ islets. SA-β-gal was not produced in 4-week-old A) male or 7-week-old B) female S64F MafA Het islets, but was in A) males by 7 weeks. (A, C) The SA-β-gal in 7 week mutant islets was of similar intensity to 10 - 12 month-old WT mouse islets. **p<0.01

References

Aguayo-Mazzucato, C., Andle, J., Lee, T.B., Jr., Midha, A., Talemal, L., Chipashvili, V., Hollister-Lock, J., van Deursen, J., Weir, G., and Bonner-Weir, S. (2019). Acceleration of beta Cell Aging Determines Diabetes and Senolysis Improves Disease Outcomes. Cell Metab *30*, 129-142 e124.

Aguayo-Mazzucato, C., Koh, A., El Khattabi, I., Li, W.C., Toschi, E., Jermendy, A., Juhl, K., Mao, K., Weir, G.C., Sharma, A., et al. (2011). Mafa expression enhances glucose-responsive insulin secretion in neonatal rat beta cells. Diabetologia *54*, 583-593.

Ahlgren, U., Jonsson, J., Jonsson, L., Simu, K., and Edlund, H. (1998). beta-cell-specific inactivation of the mouse Ipf1/Pdx1 gene results in loss of the beta-cell phenotype and maturity onset diabetes. Genes Dev *12*, 1763-1768.

Anders, S., Pyl, P.T., and Huber, W. (2015). HTSeq--a Python framework to work with high-throughput sequencing data. Bioinformatics *31*, 166-169.

Arda, H.E., Li, L., Tsai, J., Torre, E.A., Rosli, Y., Peiris, H., Spitale, R.C., Dai, C., Gu, X., Qu, K., et al. (2016). Age-Dependent Pancreatic Gene Regulation Reveals Mechanisms Governing Human beta Cell Function. Cell Metab *23*, 909-920.

Arrojo, E.D.R., Lev-Ram, V., Tyagi, S., Ramachandra, R., Deerinck, T., Bushong, E., Phan, S., Orphan, V., Lechene, C., Ellisman, M.H., et al. (2019). Age Mosaicism across Multiple Scales in Adult Tissues. Cell Metab *30*, 343-351 e343.

Artner, I., Hang, Y., Guo, M., Gu, G., and Stein, R. (2008). MafA is a dedicated activator of the insulin gene in vivo. J Endocrinol *198*, 271-279.

Artner, I., Hang, Y., Mazur, M., Yamamoto, T., Guo, M., Lindner, J., Magnuson, M.A., and Stein, R. (2010). MafA and MafB regulate genes critical to beta-cells in a unique temporal manner. Diabetes *59*, 2530-2539.

Baker, D.J., Childs, B.G., Durik, M., Wijers, M.E., Sieben, C.J., Zhong, J., Saltness, R.A., Jeganathan, K.B., Verzosa, G.C., Pezeshki, A., et al. (2016). Naturally occurring p16(Ink4a)-positive cells shorten healthy lifespan. Nature *530*, 184-189.

Baker, D.J., Wijshake, T., Tchkonia, T., LeBrasseur, N.K., Childs, B.G., van de Sluis, B., Kirkland, J.L., and van Deursen, J.M. (2011). Clearance of p16Ink4a-positive senescent cells delays ageing-associated disorders. Nature *479*, 232-236.

Banerjee, R.R., Cyphert, H.A., Walker, E.M., Chakravarthy, H., Peiris, H., Gu, X., Liu, Y., Conrad, E., Goodrich, L., Stein, R.W., et al. (2016). Gestational Diabetes Mellitus From Inactivation of Prolactin Receptor and MafB in Islet beta-Cells. Diabetes *65*, 2331-2341.

Barbetti, F., and D'Annunzio, G. (2018). Genetic causes and treatment of neonatal diabetes and early childhood diabetes. Best Pract Res Clin Endocrinol Metab *32*, 575-591.

Basisty, N., Meyer, J.G., and Schilling, B. (2018). Protein Turnover in Aging and Longevity. Proteomics *18*, e1700108.

Bergsten, P., Grapengiesser, E., Gylfe, E., Tengholm, A., and Hellman, B. (1994). Synchronous oscillations of cytoplasmic Ca2+ and insulin release in glucose-stimulated pancreatic islets. J Biol Chem *269*, 8749-8753.

Blum, B., Roose, A.N., Barrandon, O., Maehr, R., Arvanites, A.C., Davidow, L.S., Davis, J.C., Peterson, Q.P., Rubin, L.L., and Melton, D.A. (2014). Reversal of beta cell de-differentiation by a small molecule inhibitor of the TGFbeta pathway. Elife *3*, e02809.

Bolger, A.M., Lohse, M., and Usadel, B. (2014). Trimmomatic: a flexible trimmer for Illumina sequence data. Bioinformatics *30*, 2114-2120.

Bosco, D., Armanet, M., Morel, P., Niclauss, N., Sgroi, A., Muller, Y.D., Giovannoni, L., Parnaud, G., and Berney, T. (2010). Unique arrangement of alpha- and beta-cells in human islets of Langerhans. Diabetes *59*, 1202-1210.

Brissova, M., Fowler, M.J., Nicholson, W.E., Chu, A., Hirshberg, B., Harlan, D.M., and Powers, A.C. (2005). Assessment of human pancreatic islet architecture and composition by laser scanning confocal microscopy. J Histochem Cytochem *53*, 1087-1097.
Butler, P.C., Meier, J.J., Butler, A.E., and Bhushan, A. (2007). The replication of beta cells in normal physiology, in disease and for therapy. Nat Clin Pract Endocrinol Metab *3*, 758-768.
Cabrera, O., Berman, D.M., Kenyon, N.S., Ricordi, C., Berggren, P.O., and Caicedo, A. (2006). The unique cytoarchitecture of human pancreatic islets has implications for islet cell function. Proc Natl Acad Sci U S A *103*, 2334-2339.
Campisi, J. (2014). The beginning of the end. Nature *505*, 35-36.
Campisi, J., and d'Adda di Fagagna, F. (2007). Cellular senescence: when bad things happen to good cells. Nat Rev Mol Cell Biol *8*, 729-740.
Camunas-Soler, J., Dai, X., Hang, Y., Bautista, A., Lyon, J., Suzuki, K., Kim, S., Quake, S., MacDonald, P. (2019). Pancreas Patch-Seq links physiologic dysfunction in diabetes to single-cell transcriptomic phenotypes. bioRxiv.
Chang, J., Wang, Y., Shao, L., Laberge, R.M., Demaria, M., Campisi, J., Janakiraman, K., Sharpless, N.E., Ding, S., Feng, W., et al. (2016). Clearance of senescent cells by ABT263 rejuvenates aged hematopoietic stem cells in mice. Nat Med *22*, 78-83.
Chen, C., Shiota, C., Agostinelli, G., Ridley, D., Jiang, Y., Ma, J., Prasadan, K., Xiao, X., and Gittes, G.K. (2019). Evidence of a developmental origin for beta-cell heterogeneity using a dual lineage-tracing technology. Development *146*.
Childs, B.G., Baker, D.J., Wijshake, T., Conover, C.A., Campisi, J., and van Deursen, J.M. (2016). Senescent intimal foam cells are deleterious at all stages of atherosclerosis. Science *354*, 472-477.
Conrad, E., Dai, C., Spaeth, J., Guo, M., Cyphert, H.A., Scoville, D., Carroll, J., Yu, W.M., Goodrich, L.V., Harlan, D.M., et al. (2016). The MAFB transcription factor impacts islet alpha-cell function in rodents and represents a unique signature of primate islet beta-cells. Am J Physiol Endocrinol Metab *310*, E91-E102.
Coppe, J.P., Desprez, P.Y., Krtolica, A., and Campisi, J. (2010). The senescence-associated secretory phenotype: the dark side of tumor suppression. Annu Rev Pathol *5*, 99-118.
Cyphert, H.A., Walker, E.M., Hang, Y., Dhawan, S., Haliyur, R., Bonatakis, L., Avrahami, D., Brissova, M., Kaestner, K.H., Bhushan, A., et al. (2019). Examining How the MAFB Transcription Factor Affects Islet beta-Cell Function Postnatally. Diabetes *68*, 337-348.
Dadi, P.K., Luo, B., Vierra, N.C., and Jacobson, D.A. (2015). TASK-1 Potassium Channels Limit Pancreatic alpha-Cell Calcium Influx and Glucagon Secretion. Mol Endocrinol *29*, 777-787.
Dai, C., Brissova, M., Hang, Y., Thompson, C., Poffenberger, G., Shostak, A., Chen, Z., Stein, R., and Powers, A.C. (2012). Islet-enriched gene expression and glucose-induced insulin secretion in human and mouse islets. Diabetologia *55*, 707-718.
Fang, L., Igarashi, M., Leung, J., Sugrue, M.M., Lee, S.W., and Aaronson, S.A. (1999). p21Waf1/Cip1/Sdi1 induces permanent growth arrest with markers of replicative senescence in human tumor cells lacking functional p53. Oncogene *18*, 2789-2797.
Fiaschi-Taesch, N.M., Salim, F., Kleinberger, J., Troxell, R., Cozar-Castellano, I., Selk, K., Cherok, E., Takane, K.K., Scott, D.K., and Stewart, A.F. (2010). Induction of human beta-cell proliferation and engraftment using a single G1/S regulatory molecule, cdk6. Diabetes *59*, 1926-1936.
Franceschi, C., Garagnani, P., Parini, P., Giuliani, C., and Santoro, A. (2018). Inflammaging: a new immune-metabolic viewpoint for age-related diseases. Nat Rev Endocrinol *14*, 576-590.
Franklin, I., Gromada, J., Gjinovci, A., Theander, S., and Wollheim, C.B. (2005). Beta-cell secretory products activate alpha-cell ATP-dependent potassium channels to inhibit glucagon release. Diabetes *54*, 1808-1815.
Gale, E.A. (2002). Can we change the course of beta-cell destruction in type 1 diabetes? N Engl J Med *346*, 1740-1742.

Gannon, M., Kulkarni, R.N., Tse, H.M., and Mauvais-Jarvis, F. (2018). Sex differences underlying pancreatic islet biology and its dysfunction. Mol Metab *15*, 82-91.
Gilbert, J.M., and Blum, B. (2018). Synaptotagmins Tweak Functional beta Cell Maturation. Dev Cell *45*, 284-286.
Golson, M.L., and Kaestner, K.H. (2017). Epigenetics in formation, function, and failure of the endocrine pancreas. Mol Metab *6*, 1066-1076.
Gorgoulis, V., Adams, P.D., Alimonti, A., Bennett, D.C., Bischof, O., Bishop, C., Campisi, J., Collado, M., Evangelou, K., Ferbeyre, G., et al. (2019). Cellular Senescence: Defining a Path Forward. Cell *179*, 813-827.
Greenhill, C. (2019). Regulating metabolism and ageing - the role of PI3K. Nat Rev Endocrinol *15*, 376-377.
Guo, S., Burnette, R., Zhao, L., Vanderford, N.L., Poitout, V., Hagman, D.K., Henderson, E., Ozcan, S., Wadzinski, B.E., and Stein, R. (2009). The stability and transactivation potential of the mammalian MafA transcription factor are regulated by serine 65 phosphorylation. J Biol Chem *284*, 759-765.
Guo, S., Dai, C., Guo, M., Taylor, B., Harmon, J.S., Sander, M., Robertson, R.P., Powers, A.C., and Stein, R. (2013). Inactivation of specific beta cell transcription factors in type 2 diabetes. J Clin Invest *123*, 3305-3316.
Guo, S., Vanderford, N.L., and Stein, R. (2010). Phosphorylation within the MafA N terminus regulates C-terminal dimerization and DNA binding. J Biol Chem *285*, 12655-12661.
Han, S.I., Aramata, S., Yasuda, K., and Kataoka, K. (2007). MafA stability in pancreatic beta cells is regulated by glucose and is dependent on its constitutive phosphorylation at multiple sites by glycogen synthase kinase 3. Mol Cell Biol *27*, 6593-6605.
Hang, Y., and Stein, R. (2011). MafA and MafB activity in pancreatic beta cells. Trends Endocrinol Metab *22*, 364-373.
Hang, Y., Yamamoto, T., Benninger, R.K., Brissova, M., Guo, M., Bush, W., Piston, D.W., Powers, A.C., Magnuson, M., Thurmond, D.C., et al. (2014). The MafA transcription factor becomes essential to islet beta-cells soon after birth. Diabetes *63*, 1994-2005.
Harmon, J.S., Stein, R., and Robertson, R.P. (2005). Oxidative stress-mediated, post-translational loss of MafA protein as a contributing mechanism to loss of insulin gene expression in glucotoxic beta cells. J Biol Chem *280*, 11107-11113.
Helman, A., Klochendler, A., Azazmeh, N., Gabai, Y., Horwitz, E., Anzi, S., Swisa, A., Condiotti, R., Granit, R.Z., Nevo, Y., et al. (2016). p16(Ink4a)-induced senescence of pancreatic beta cells enhances insulin secretion. Nat Med *22*, 412-420.
Henquin, J.C., Dufrane, D., and Nenquin, M. (2006). Nutrient control of insulin secretion in isolated normal human islets. Diabetes *55*, 3470-3477.
Herranz, N., and Gil, J. (2018). Mechanisms and functions of cellular senescence. J Clin Invest *128*, 1238-1246.
Iacovazzo, D., Flanagan, S.E., Walker, E., Quezado, R., de Sousa Barros, F.A., Caswell, R., Johnson, M.B., Wakeling, M., Brandle, M., Guo, M., et al. (2018). MAFA missense mutation causes familial insulinomatosis and diabetes mellitus. Proc Natl Acad Sci U S A *115*, 1027-1032.
Jacobson, D.A., and Shyng, S.L. (2020). Ion Channels of the Islets in Type 2 Diabetes. J Mol Biol *432*, 1326-1346.
Kabir, T.D., Leigh, R.J., Tasena, H., Mellone, M., Coletta, R.D., Parkinson, E.K., Prime, S.S., Thomas, G.J., Paterson, I.C., Zhou, D., et al. (2016). A miR-335/COX-2/PTEN axis regulates the secretory phenotype of senescent cancer-associated fibroblasts. Aging (Albany NY) *8*, 1608-1635.
Kalwat, M.A., and Cobb, M.H. (2017). Mechanisms of the amplifying pathway of insulin secretion in the beta cell. Pharmacol Ther *179*, 17-30.
Kim, D., Langmead, B., and Salzberg, S.L. (2015). HISAT: a fast spliced aligner with low memory requirements. Nat Methods *12*, 357-360.

Kurz, D.J., Decary, S., Hong, Y., and Erusalimsky, J.D. (2000). Senescence-associated (beta)-galactosidase reflects an increase in lysosomal mass during replicative ageing of human endothelial cells. J Cell Sci *113 (Pt 20)*, 3613-3622.
Love, M.I., Huber, W., and Anders, S. (2014). Moderated estimation of fold change and dispersion for RNA-seq data with DESeq2. Genome Biol *15*, 550.
Luan, C., Ye, Y., Singh, T., Barghouth, M., Eliasson, L., Artner, I., Zhang, E., and Renstrom, E. (2019). The calcium channel subunit gamma-4 is regulated by MafA and necessary for pancreatic beta-cell specification. Commun Biol *2*, 106.
Madsen, O.D., Jensen, J., Petersen, H.V., Pedersen, E.E., Oster, A., Andersen, F.G., Jorgensen, M.C., Jensen, P.B., Larsson, L.I., and Serup, P. (1997). Transcription factors contributing to the pancreatic beta-cell phenotype. Horm Metab Res *29*, 265-270.
Mancini, M., Saintigny, G., Mahe, C., Annicchiarico-Petruzzelli, M., Melino, G., and Candi, E. (2012). MicroRNA-152 and -181a participate in human dermal fibroblasts senescence acting on cell adhesion and remodeling of the extra-cellular matrix. Aging (Albany NY) *4*, 843-853.
Martin, N., and Bernard, D. (2018). Calcium signaling and cellular senescence. Cell Calcium *70*, 16-23.
Martinez, M.N., Emfinger, C.H., Overton, M., Hill, S., Ramaswamy, T.S., Cappel, D.A., Wu, K., Fazio, S., McDonald, W.H., Hachey, D.L., et al. (2012). Obesity and altered glucose metabolism impact HDL composition in CETP transgenic mice: a role for ovarian hormones. J Lipid Res *53*, 379-389.
Pan, F.C., Brissova, M., Powers, A.C., Pfaff, S., and Wright, C.V. (2015). Inactivating the permanent neonatal diabetes gene Mnx1 switches insulin-producing beta-cells to a delta-like fate and reveals a facultative proliferative capacity in aged beta-cells. Development *142*, 3637-3648.
Pan, F.C., and Wright, C. (2011). Pancreas organogenesis: from bud to plexus to gland. Dev Dyn *240*, 530-565.
Raum, J.C., Gerrish, K., Artner, I., Henderson, E., Guo, M., Sussel, L., Schisler, J.C., Newgard, C.B., and Stein, R. (2006). FoxA2, Nkx2.2, and PDX-1 regulate islet beta-cell-specific mafA expression through conserved sequences located between base pairs -8118 and -7750 upstream from the transcription start site. Mol Cell Biol *26*, 5735-5743.
Raum, J.C., Hunter, C.S., Artner, I., Henderson, E., Guo, M., Elghazi, L., Sosa-Pineda, B., Ogihara, T., Mirmira, R.G., Sussel, L., et al. (2010). Islet beta-cell-specific MafA transcription requires the 5'-flanking conserved region 3 control domain. Mol Cell Biol *30*, 4234-4244.
Rocques, N., Abou Zeid, N., Sii-Felice, K., Lecoin, L., Felder-Schmittbuhl, M.P., Eychene, A., and Pouponnot, C. (2007). GSK-3-mediated phosphorylation enhances Maf-transforming activity. Mol Cell *28*, 584-597.
Russell, R., Carnese, P., Hennings, T., Walker, E., Russ, H., Giacometti, S., Stein, R., Hebrok, M. (2020). Genome editing in hPSCs reveals an important role for MAFB in human pancreatic endocrine
cell specification. Nature Communications, In Press.
Sampathkumar, N.K., Bravo, J.I., Chen, Y., Danthi, P.S., Donahue, E.K., Lai, R.W., Lu, R., Randall, L.T., Vinson, N., and Benayoun, B.A. (2019). Widespread sex dimorphism in aging and age-related diseases. Hum Genet.
Scharfmann, R., Pechberty, S., Hazhouz, Y., von Bulow, M., Bricout-Neveu, E., Grenier-Godard, M., Guez, F., Rachdi, L., Lohmann, M., Czernichow, P., et al. (2014). Development of a conditionally immortalized human pancreatic beta cell line. J Clin Invest *124*, 2087-2098.
Schultz, L.B., Chehab, N.H., Malikzay, A., and Halazonetis, T.D. (2000). p53 binding protein 1 (53BP1) is an early participant in the cellular response to DNA double-strand breaks. J Cell Biol *151*, 1381-1390.
Scoville, D.W., Cyphert, H.A., Liao, L., Xu, J., Reynolds, A., Guo, S., and Stein, R. (2015). MLL3 and MLL4 Methyltransferases Bind to the MAFA and MAFB Transcription Factors to Regulate Islet beta-Cell Function. Diabetes *64*, 3772-3783.

Shih, H.P., Wang, A., and Sander, M. (2013). Pancreas organogenesis: from lineage determination to morphogenesis. Annu Rev Cell Dev Biol *29*, 81-105.
Thompson, P.J., Shah, A., Ntranos, V., Van Gool, F., Atkinson, M., and Bhushan, A. (2019). Targeted Elimination of Senescent Beta Cells Prevents Type 1 Diabetes. Cell Metab *29*, 1045-1060 e1010.
Tyrberg, B., Andersson, A., and Borg, L.A. (2001). Species differences in susceptibility of transplanted and cultured pancreatic islets to the beta-cell toxin alloxan. Gen Comp Endocrinol *122*, 238-251.
van der Meulen, T., Donaldson, C.J., Caceres, E., Hunter, A.E., Cowing-Zitron, C., Pound, L.D., Adams, M.W., Zembrzycki, A., Grove, K.L., and Huising, M.O. (2015). Urocortin3 mediates somatostatin-dependent negative feedback control of insulin secretion. Nat Med *21*, 769-776.
van Deursen, J.M. (2014). The role of senescent cells in ageing. Nature *509*, 439-446.
Zhang, C., Moriguchi, T., Kajihara, M., Esaki, R., Harada, A., Shimohata, H., Oishi, H., Hamada, M., Morito, N., Hasegawa, K., et al. (2005). MafA is a key regulator of glucose-stimulated insulin secretion. Mol Cell Biol *25*, 4969-4976.

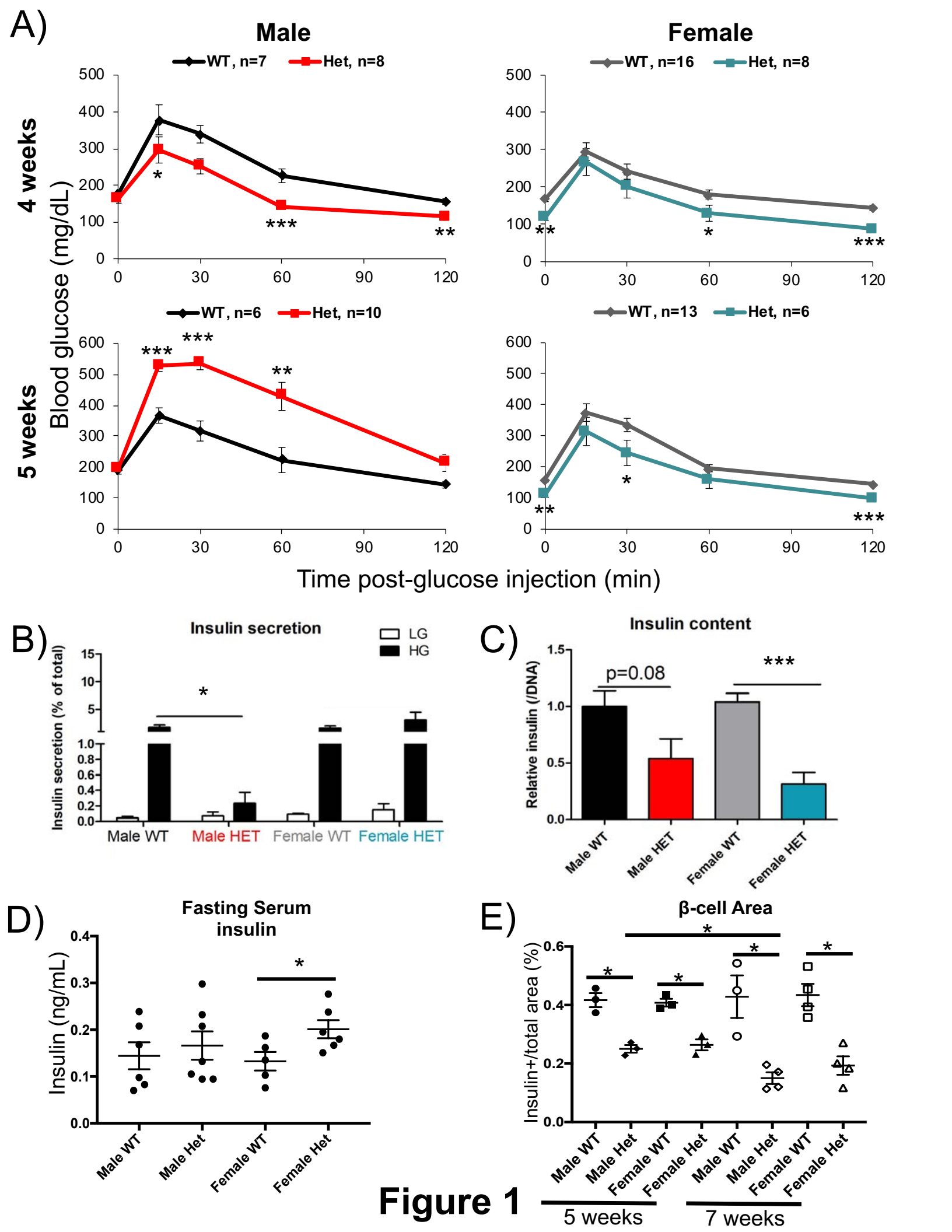
A)
Male
Female
WT, n=7
Het, n=8
WT, n=16
Het, n=8
WT, n=6
Het, n=10
WT, n=13
Het, n=6
4 weeks
5 weeks
Blood glucose (mg/dL)
Time post-glucose injection (min)
B)
Insulin secretion
LG
HG
Insulin secretion (% of total)
Male WT
Male HET
Female WT
Female HET
C)
Insulin content
Relative insulin (/DNA)
p=0.08
Male WT
Male HET
Female WT
Female HET
D)
Fasting Serum insulin
Insulin (ng/mL)
Male WT
Male Het
Female WT
Female Het
E)
β-cell Area
Insulin+/total area (%)
Male WT
Male Het
Female WT
Female Het
5 weeks
7 weeks

Figure 1

A)

Male

3 weeks | 4 weeks | 5 weeks | 6 weeks | 7 weeks

MafA Insulin

WT

Het

B)

Female

3 weeks | 4 weeks | 5 weeks | 6 weeks | 7 weeks

MafA Insulin

WT

Het

C)

MafA

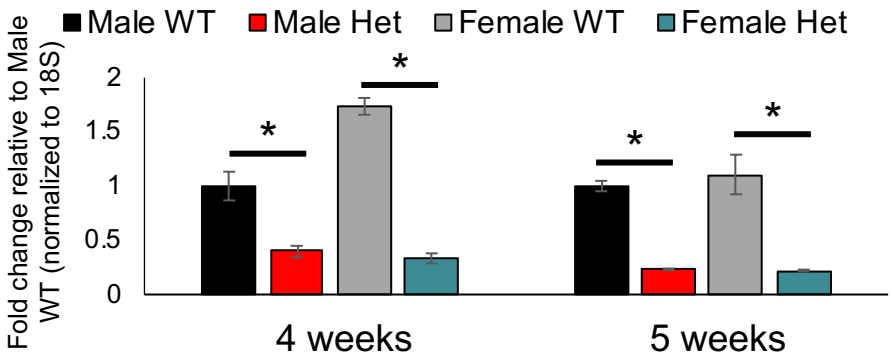

Figure 2

A)

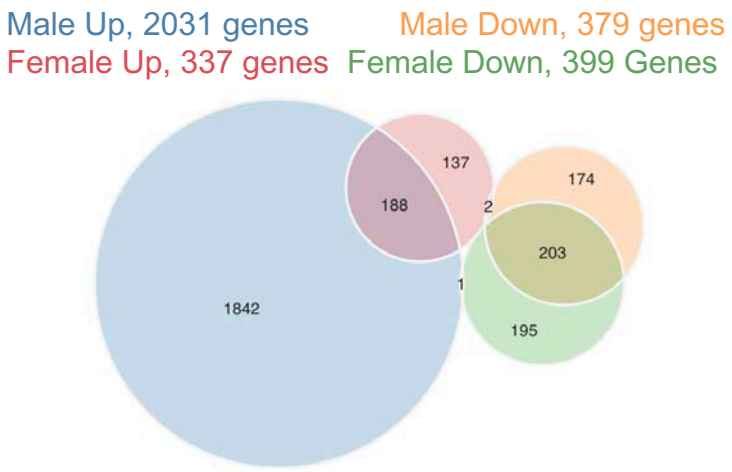

B)

GO: Molecular function

Index	Name	P-value	Adjusted p-value	Odds Ratio
1	voltage-gated potassium channel activity (GO:0005249)	0.0002574	0.2963	4.81
2	potassium channel activity (GO:0005267)	0.0007727	0.4447	4.09
3	voltage-gated cation channel activity (GO:0022843)	0.0007727	0.2964	4.09
4	delayed rectifier potassium channel activity (GO:0005251)	0.002320	0.6677	7.06
5	alpha-N-acetylneuraminate alpha-2,8-sialyltransferase activity (GO:0003828)	0.005428	1.000	17.05
6	G-protein coupled receptor activity (GO:0004930)	0.006546	1.000	2.30
7	opioid receptor activity (GO:0004985)	0.007502	1.000	14.61
8	sialyltransferase activity (GO:0008373)	0.007592	1.000	7.31
9	GABA receptor activity (GO:0016917)	0.007592	0.9709	7.31
10	extracellular ligand-gated ion channel activity (GO:0005230)	0.01863	1.000	3.93

C)

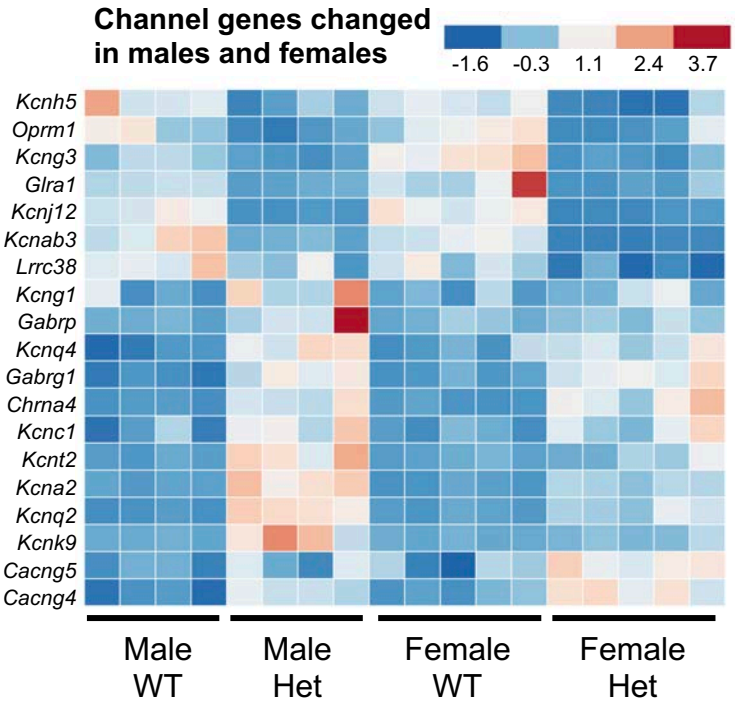

D)

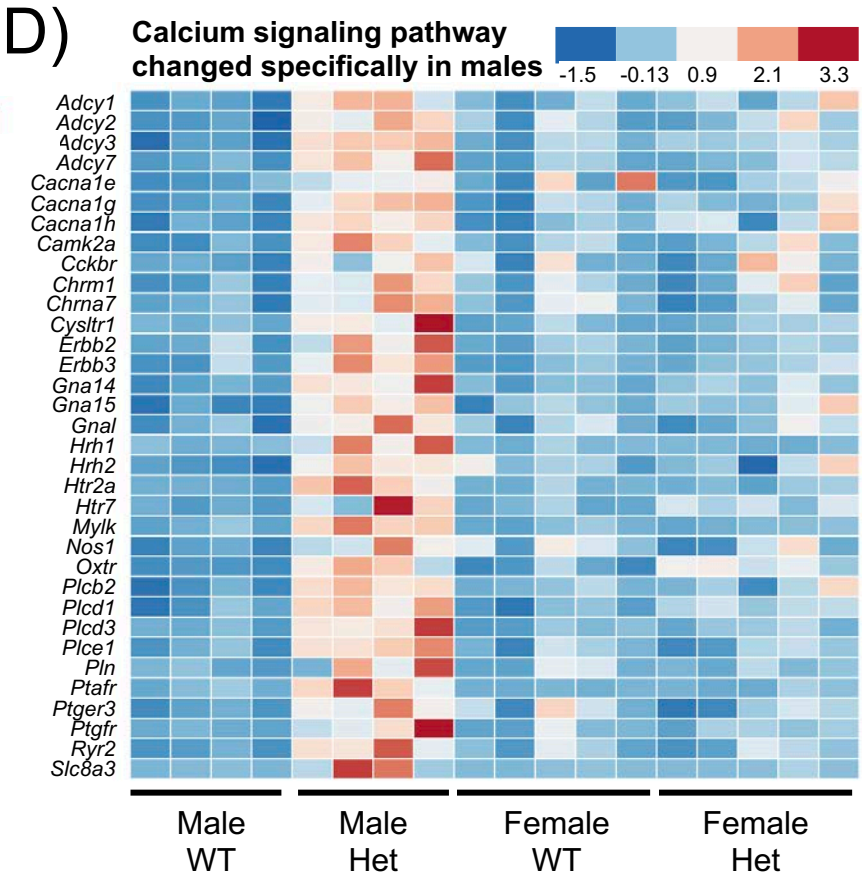

Figure 3

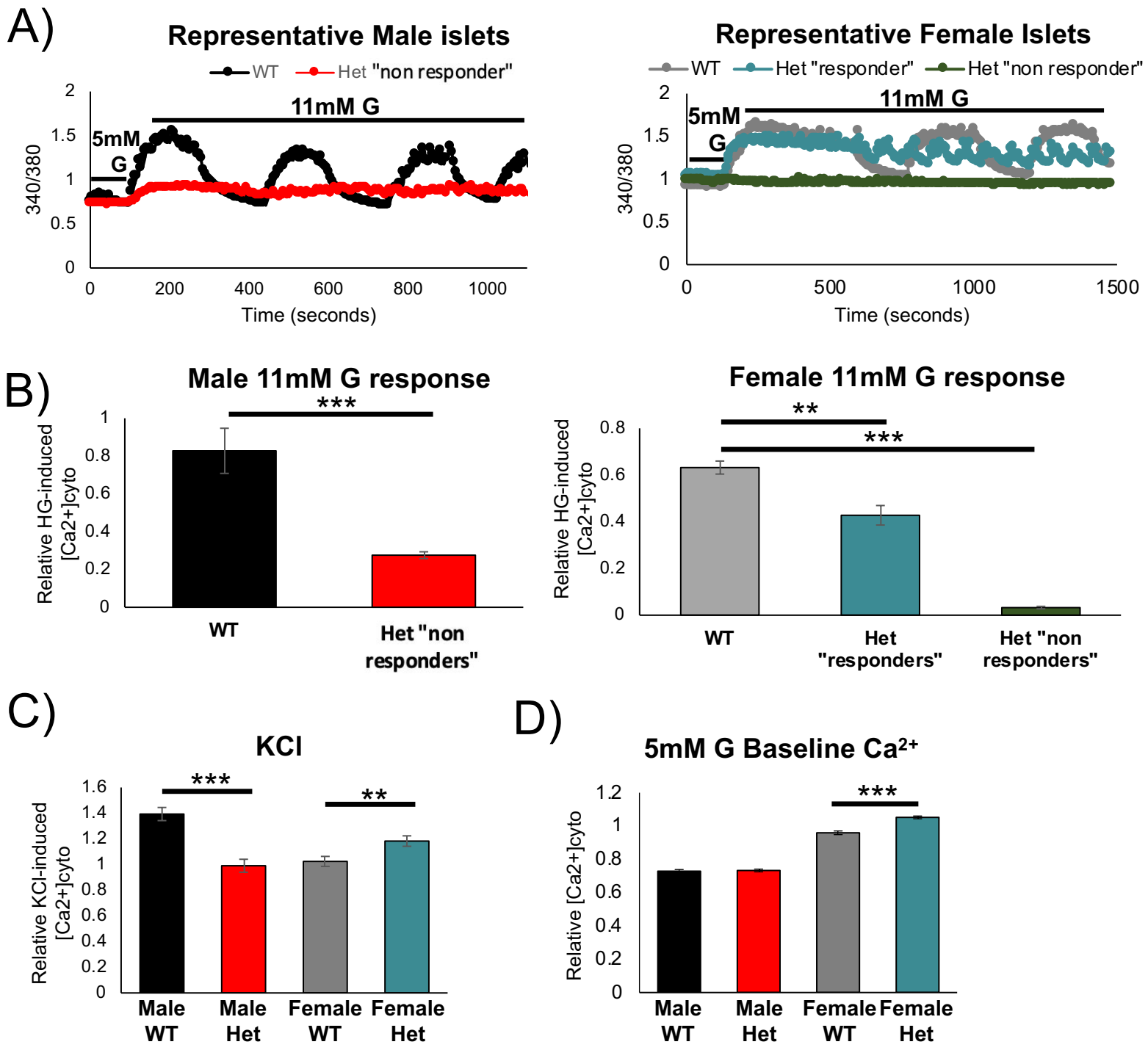
A)
Representative Male islets
WT
Het "non responder"
11mM G
5mM G
340/380
Time (seconds)
Representative Female Islets
WT
Het "responder"
Het "non responder"
11mM G
5mM G
340/380
Time (seconds)
B)
Male 11mM G response
***
Relative HG-induced [Ca2+]cyto
WT
Het "non responders"
Female 11mM G response
**
***
Relative HG-induced [Ca2+]cyto
WT
Het "responders"
Het "non responders"
C)
KCl
***
**
Relative KCl-induced [Ca2+]cyto
Male WT
Male Het
Female WT
Female Het
D)
5mM G Baseline Ca2+
***
Relative [Ca2+]cyto
Male WT
Male Het
Female WT
Female Het

Figure 4

A) **KEGG analysis**

Index	Name	P-value	Adjusted p-value	Z-score
1	Protein digestion and absorption_Homo sapiens_hsa04974	2.396e-9	5.055e-7	-1.72
2	ECM-receptor interaction_Homo sapiens_hsa04512	1.786e-7	0.00001884	-1.68
3	Cytokine-cytokine receptor interaction_Homo sapiens_hsa04060	0.000003286	0.0002311	-1.83
4	PI3K-Akt signaling pathway_Homo sapiens_hsa04151	0.00001506	0.0006357	-1.96
5	Arachidonic acid metabolism_Homo sapiens_hsa00590	0.00001060	0.0005591	-1.89
6	Calcium signaling pathway_Homo sapiens_hsa04020	0.00002454	0.0008628	-1.83
7	Focal adhesion_Homo sapiens_hsa04510	0.00003833	0.001155	-1.77
8	AGE-RAGE signaling pathway in diabetic complications_Homo sapiens_hsa04933	0.00006126	0.001293	-1.80
9	Malaria_Homo sapiens_hsa05144	0.00005057	0.001293	-1.64
10	Amoebiasis_Homo sapiens_hsa05146	0.00005514	0.001293	-1.65

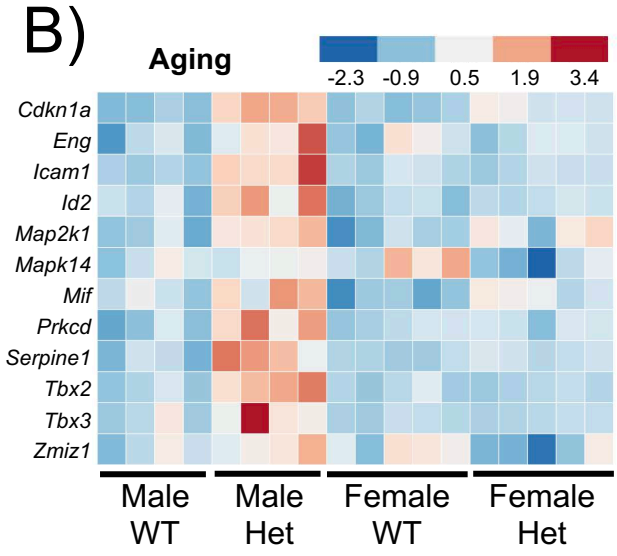

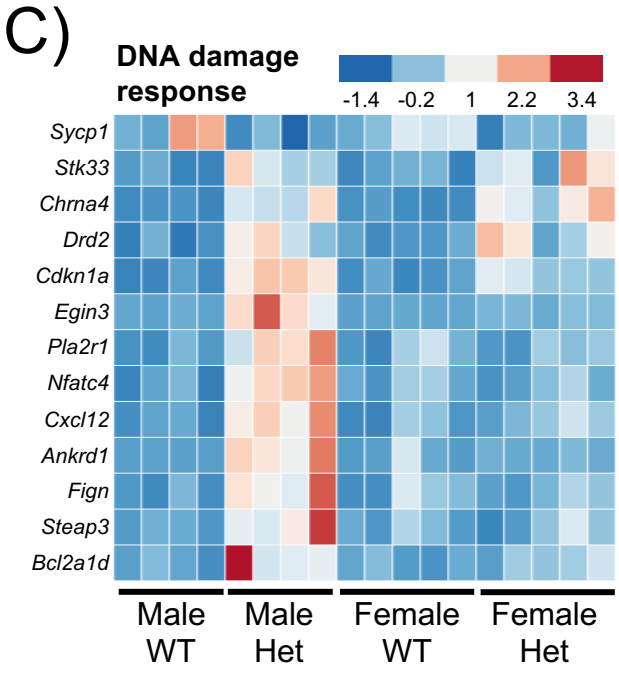

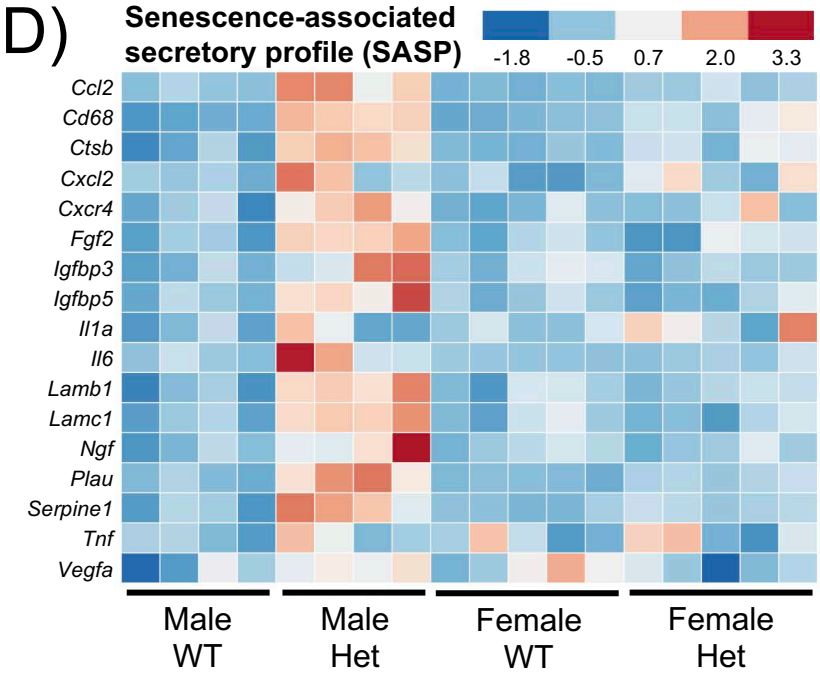

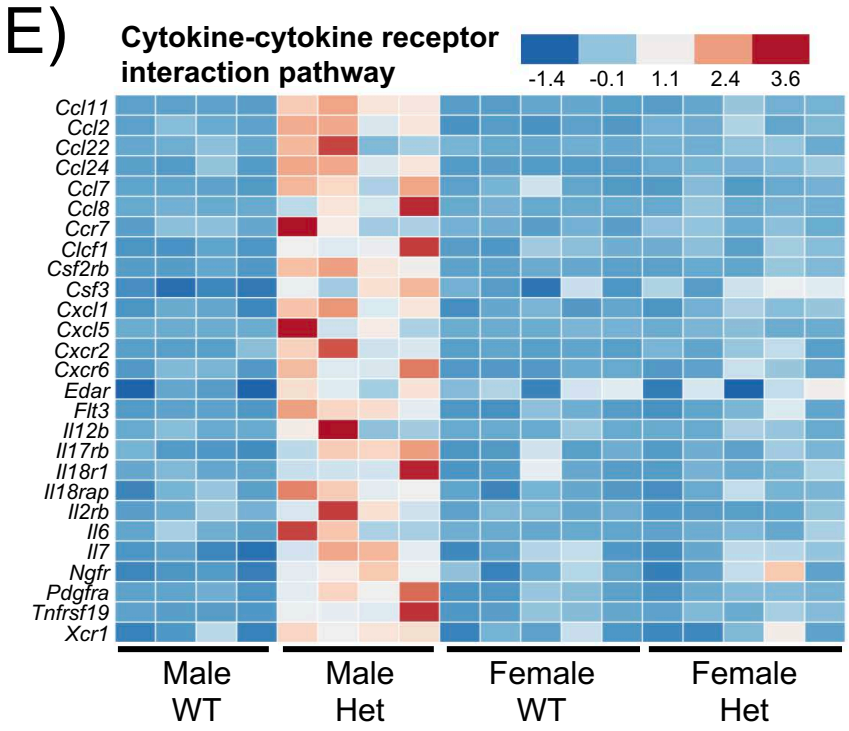

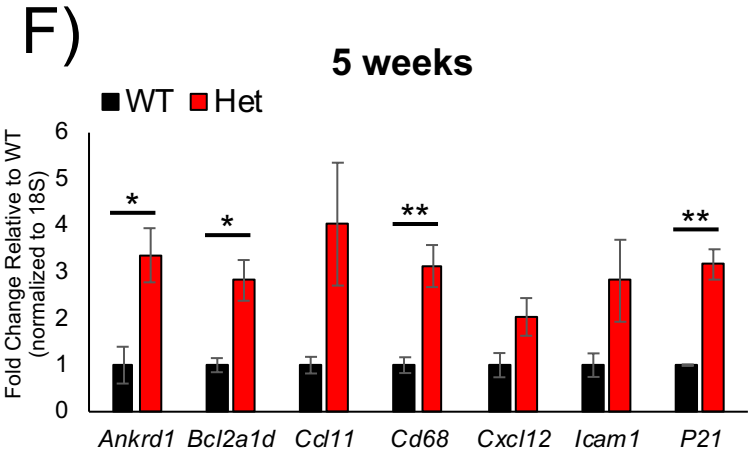

Figure 5

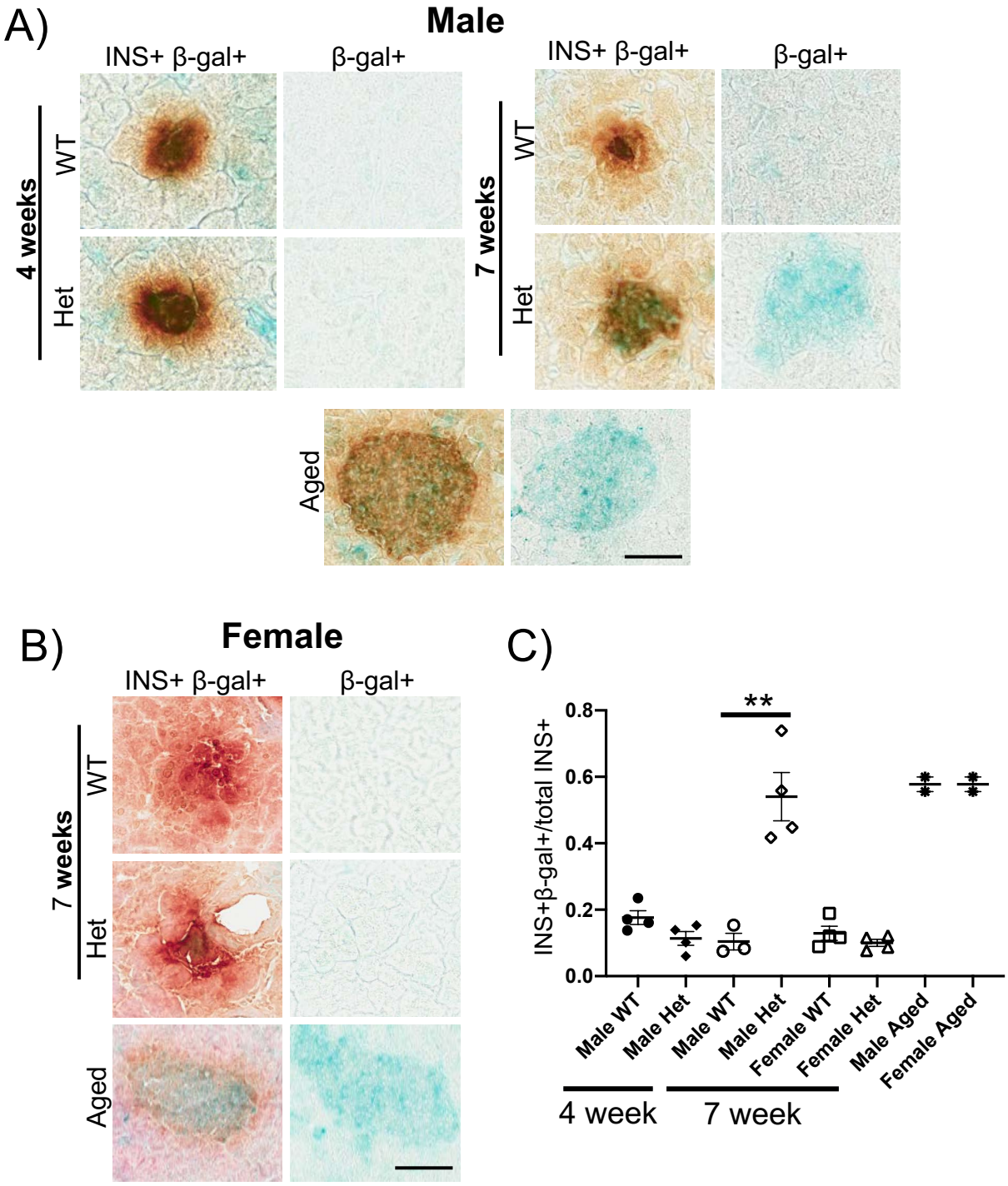
A)
Male
INS+ β-gal+
β-gal+
INS+ β-gal+
β-gal+
4 weeks
WT
Het
7 weeks
WT
Het
Aged
B)
Female
INS+ β-gal+
β-gal+
7 weeks
WT
Het
Aged
C)
INS+β-gal+/total INS+
0.8
0.6
0.4
0.2
0.0
**
Male WT
Male Het
Male WT
Male Het
Female WT
Female Het
Male Aged
Female Aged
4 week
7 week

Figure 6